Proceedings of 2004 IEEE/RSJ International Conference on
Intelligent Robots and Systems
September 28 - October 2, 2004, Sendai, Japan

On the Stability of Indirect ZMP Controller for Biped Robot Systems

Youngjin Choi, Bum-Jae You and Sang-Rok Oh
Intelligent Robotics Research Center
Korea Institute of Science & Technology (KIST)
Seoul, 136-791, Korea
Email: {cyj, ybj, sroh}@kist.re.kr

Abstract— **This paper proposes the indirect zero momentum position (ZMP) controller for biped robot systems and proves its disturbance input-to-state stability (ISS). The ZMP control has been used as a standard method for stable walking control of biped robot systems. Since the ZMP information consists of position and acceleration of the center of gravity (COG) for a biped robot system, the ZMP can be indirectly controlled by the motion of COG. In this paper, the reference COG Planner is developed by solving the reference ZMP differential equation. The indirect ZMP controller is proposed to derive the desired motion of COG from the reference ZMP trajectory and the COG error (the difference between the reference and real COG). The ISS of the proposed indirect ZMP controller is proved for the simplified biped robot model. The robustness of the proposed indirect ZMP controller is shown in simulation.**

I. Introduction

The zero momentum position (ZMP) control is the most important factor in implementing stable biped robot walking. If the ZMP is located in the region of supporting sole, then the robot will not fall down during walking. To implement stable robot walking, ZMP planning methods were first suggested by using the inverted pendulum model[1] and the fast fourier transformation[2]. In order to compensate the error between the planned and actual ZMP, various ZMP control methods were suggested: for example, direct and indirect ZMP control methods[3], [4], impedance control[5] and balance control[6]. Recently, running pattern generation methods were suggested in [7], [8]. Moreover, whole body planning of humanoid robot based on ZMP were suggested in [9], [10]. Despite many references to biped walking control methods, research on the stability of biped walking controllers is still lacking. The exponential stability of periodic walking motion was partially proved for a planar biped robot in [11], [12].

In this paper, we will propose the indirect ZMP control method and prove its disturbance input-to-state stability (ISS). Due to the modelling uncertainties and the complexity of the full dynamics for a biped walking robot, we will represent the dynamic walking robot as a simple rolling sphere model on a constraint surface. This paper is organized as follows: section II introduces a simplified model for a biped walking robot, section III proposes the COG trajectory planning method from the reference ZMP trajectory, section IV proves the ISS of indirect ZMP control for the simplified biped model and section V concludes the paper.

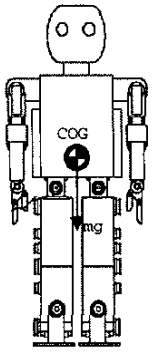

Fig. 1. Biped Walking Robot

II. Simplified Model for Dynamic Walking Robot

The biped walking mechanism is an essential part of humanoid as shown in Figure 1. Since humanoid legs have high degrees of freedom (DOF) for human-like walking, it is difficult to use their dynamics to design controller and to analyze stability. Therefore, we will simplify the walking related dynamics of biped robot as the equation of motion for a point mass at COG.

First, let us assume that the motion of COG is constrained on the surface $z = c_z$. Then the rolling sphere (mass = m) model on constraint surface ($z = c_z$) can be obtained as the simplified model for biped walking robot as shown in Figure 2. In this figure, the motion of the rolling sphere on a massless plate is described by the position of COG, (c_x, c_y, c_z), and the ZMP is described by the position on the ground, $(p_x, p_y, 0)$. The joint configurations of the supporting leg are determined by solving the inverse kinematics from the position of COG to the base foot position (BFP) on the ground and those of shifting leg are determined by solving the inverse kinematics from the position of COG to the shifting foot position (SFP).

Second, the equations of motion of the rolling sphere (mass = m) in Figure 2 are obtained on the plane $z = c_z$

0-7803-8463-6/04/$20.00 ©2004 IEEE

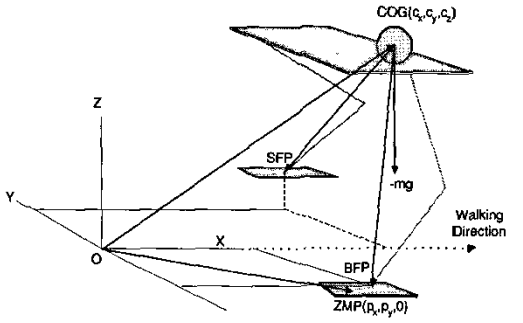

Fig. 2. Rolling Sphere Model for Dynamic Walking

as:

$$\tau_x = mgc_y - m\ddot{c}_y c_z \quad (1)$$

$$\tau_y = -mgc_x + m\ddot{c}_x c_z \quad (2)$$

$$\tau_z = -m\ddot{c}_x c_y + m\ddot{c}_y c_x \quad (3)$$

where g is the acceleration of gravity, c_z is a height constant and τ_i is the moment about i-coordinate axis, for $i = x, y, z$. Now, if we introduce the definition of ZMP as following forms:

$$p_x \triangleq -\frac{\tau_y}{mg} \quad (4)$$

$$p_y \triangleq \frac{\tau_x}{mg} \quad (5)$$

to two equations (1) and (2), then ZMP equations can be obtained as two differential equations:

$$p_x = c_x - \frac{c_z}{g}\ddot{c}_x \quad (6)$$

$$p_y = c_y - \frac{c_z}{g}\ddot{c}_y. \quad (7)$$

The state space realization of ZMP equations (6) and (7) can be written as:

$$\frac{d}{dt}\begin{bmatrix} c_i \\ \dot{c}_i \end{bmatrix} = \begin{bmatrix} 0 & 1 \\ g/c_z & 0 \end{bmatrix}\begin{bmatrix} c_i \\ \dot{c}_i \end{bmatrix} + \begin{bmatrix} 0 \\ -g/c_z \end{bmatrix} p_i, \quad (8)$$

for $i = x, y$. These state space equations describe the relation between the position of COG and the ZMP, and they will be used as a part of the indirect ZMP controller in the following section.

III. Reference Trajectory of COG

To implement robot walking, first of all, the stepping positions on the ground and the supporting phases should be predetermined as shown in Figure 3. In this figure, the stepping positions are generally represented as periodic functions and the supporting phases (double supporting and single supporting) are used in moving the ZMP. In a single supporting phase, the ZMP should stay in the center of the sole of supporting leg while the shifting leg is making a step. In a double supporting phase, the ZMP should be moved to the center of the sole of shifting leg. These procedures should be repeated to make stable robot walking. Also, the reference trajectory of COG should be derived from the reference ZMP in Figure 3. In this section, we develop the equations for the generation of the reference trajectory of COG.

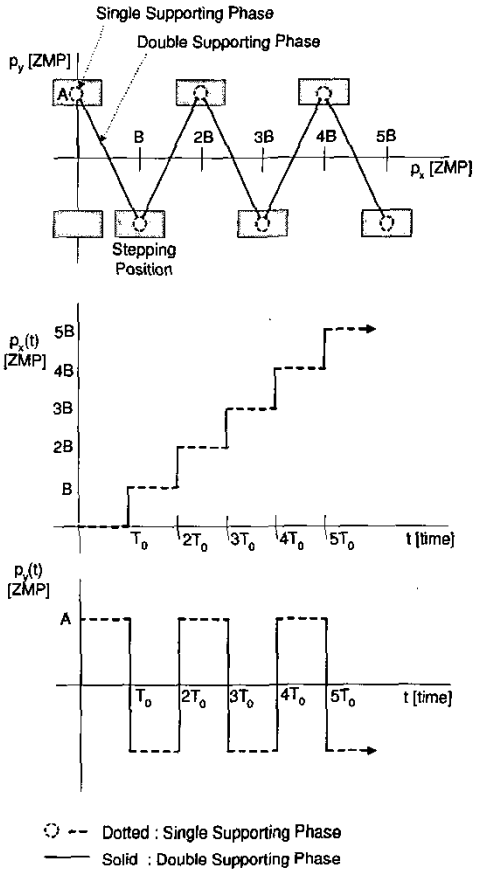

Fig. 3. The Stepping Positions and Reference ZMP $p_x^{ref}(t)$ and $p_y^{ref}(t)$

A. Exact Solution

From the equations (6) and (7), we can get the following transfer function:

$$C_i(s) = \frac{1}{1-(c_z/g)s^2}\left[P_i(s) - (c_z/g)c_i(0)s - (c_z/g)\dot{c}_i(0)\right] \quad (9)$$

for $i = x, y$, where $C_i(s)$ and $P_i(s)$ are the Laplace transformations of $c_i(t)$ and $p_i(t)$, respectively, $c_i(0)$ and $\dot{c}_i(0)$ are the initial conditions of trajectory of COG. The reference ZMP shown in Figure 3 can be expressed as:

$$p_x^{ref}(t) = B\sum_{k=1}^{\infty} 1(t - kT_0) \quad (10)$$

$$p_y^{ref}(t) = A \cdot 1(t) + 2A\sum_{k=1}^{\infty}(-1)^k \cdot 1(t - kT_0) \quad (11)$$

where $1(t - kT_0)$ is the unit-step function starting at $t = kT_0$. If we apply the Laplace transformations of the equations (10) and (11) to the equation (9) with zero initial conditions, then we get the followings:

$$\begin{aligned} C_x(s) &= \frac{1}{1-(c_z/g)s^2}\left[\frac{B}{s}e^{-T_0 s}+\frac{B}{s}e^{-2T_0 s} \right. \\ &\quad \left. +\frac{B}{s}e^{-3T_0 s}+\cdots\right] \\ C_y(s) &= \frac{1}{1-(c_z/g)s^2}\left[\frac{A}{s}-\frac{2A}{s}e^{-T_0 s} \right. \\ &\quad \left. +\frac{2A}{s}e^{-2T_0 s}-\cdots\right]. \end{aligned}$$

Now, by letting $\omega_n^2 \triangleq g/c_z$, since we know that

$$\frac{1}{1-(c_z/g)s^2}\cdot\frac{1}{s}=\frac{1}{s}-\frac{s}{s^2-\omega_n^2},$$

we get the following rearranged transfer functions:

$$\begin{aligned} C_x(s) &= B\left(\frac{1}{s}-\frac{s}{s^2-\omega_n^2}\right)e^{-T_0 s} \\ &\quad +B\left(\frac{1}{s}-\frac{s}{s^2-\omega_n^2}\right)e^{-2T_0 s} \\ &\quad +B\left(\frac{1}{s}-\frac{s}{s^2-\omega_n^2}\right)e^{-3T_0 s}+\cdots \\ C_y(s) &= A\left(\frac{1}{s}-\frac{s}{s^2-\omega_n^2}\right) \\ &\quad -2A\left(\frac{1}{s}-\frac{s}{s^2-\omega_n^2}\right)e^{-T_0 s} \\ &\quad +2A\left(\frac{1}{s}-\frac{s}{s^2-\omega_n^2}\right)e^{-2T_0 s}-\cdots \end{aligned}$$

Finally, we can obtain the exact reference trajectories of the COG by using the inverse Laplace transformations as:

$$\begin{aligned} c_x(t) &= B\left[1-cosh\ \omega_n(t-T_0)\right]\cdot 1(t-T_0)+ \\ &\quad B\left[1-cosh\ \omega_n(t-2T_0)\right]\cdot 1(t-2T_0)+ \\ &\quad B\left[1-cosh\ \omega_n(t-3T_0)\right]\cdot 1(t-3T_0)+\cdots \\ &= B\sum_{k=1}^{\infty}\left[1-cosh\ \omega_n(t-kT_0)\right]\cdot 1(t-kT_0) \\ c_y(t) &= A\left[1-cosh\ \omega_n(t)\right]- \\ &\quad 2A\left[1-cosh\ \omega_n(t-T_0)\right]\cdot 1(t-T_0)+ \\ &\quad 2A\left[1-cosh\ \omega_n(t-2T_0)\right]\cdot 1(t-2T_0)-\cdots \\ &= A\left[1-cosh\ \omega_n(t)\right]+ \\ &\quad 2A\sum_{k=1}^{\infty}(-1)^k\left[1-cosh\ \omega_n(t-kT_0)\right]\cdot 1(t-kT_0) \end{aligned}$$

Even though these reference trajectories of COG are exact solutions for ordinary differential equations (6) and (7), they are difficult to be used robustly for a real biped walking robot system since they are composed of the unbounded functions $cosh(\cdot)$. In addition, they are numerically unstable and very sensitive to the variation of ω_n. Therefore, we will suggest an alternative robust COG trajectory planning method by using the approximate solution composed of the bounded functions in the following section.

B. Planning by Approximate Solution

First, we introduce the following odd function with period T_0 from the x-directional reference ZMP $p_x^{ref}(t)$ of equation (10):

$$\begin{aligned} p'_x(t) &\triangleq p_x^{ref}(t)-\frac{B}{T_0}\left(t-\frac{T_0}{2}\right) \\ &= -\frac{B}{T_0}\left(t-\frac{T_0}{2}\right) \quad \text{and} \quad p'_x(t+T_0)=p'_x(t). \end{aligned}$$

Then, if we assume that the x-directional reference trajectory of COG has the following form by using Fourier series:

$$\begin{aligned} c_x^{ref}(t) &= \frac{B}{T_0}\left(t-\frac{T_0}{2}\right) \\ &\quad +\sum_{n=1}^{\infty}\left[a_n\cos\left(\frac{n\pi}{T_0}t\right)+b_n\sin\left(\frac{n\pi}{T_0}t\right)\right], \end{aligned}$$

then we get the following equation by applying the above equation to the ZMP differential equation (6):

$$p_x^{ref}(t)=\frac{B}{T_0}\left(t-\frac{T_0}{2}\right)+p'_x(t),$$

where

$$\begin{aligned} p'_x(t) &= \sum_{n=1}^{\infty}\left[a_n\left(1+\frac{n^2\pi^2}{T_0^2\omega_n^2}\right)\cos\left(\frac{n\pi}{T_0}t\right) \right. \\ &\quad \left. +b_n\left(1+\frac{n^2\pi^2}{T_0^2\omega_n^2}\right)\sin\left(\frac{n\pi}{T_0}t\right)\right]. \end{aligned}$$

Since above function $p'_x(t)$ is an odd function with a period T_0, the coefficients $a_n = 0$ and b_n can be obtained by solving the following equation:

$$b_n\left(1+\frac{n^2\pi^2}{T_0^2\omega_n^2}\right)=\frac{2}{T_0}\int_0^{T_0}p'_x(t)\sin\left(\frac{n\pi}{T_0}t\right)dt.$$

Finally, we get the coefficient b_n as the following form:

$$b_n=\frac{BT_0^2\omega_n^2(1+\cos n\pi)}{n\pi(T_0^2\omega_n^2+n^2\pi^2)}.$$

As a result, the x-directional reference trajectory of COG can be obtained by using the bounded function $sin(\cdot)$ as follows:

$$\begin{aligned} c_x^{ref}(t) &= \frac{B}{T_0}\left(t-\frac{T_0}{2}\right)+ \\ &\quad \sum_{n=1}^{\infty}\frac{BT_0^2\omega_n^2(1+\cos n\pi)}{n\pi(T_0^2\omega_n^2+n^2\pi^2)}\sin\left(\frac{n\pi}{T_0}t\right). \end{aligned} \quad (12)$$

Also, since the y-directional reference ZMP $p_y^{ref}(t)$ of the equation (11) is the odd function with a period T_0, we can get the following y-directional reference trajectory of COG by using the Fourier series:

$$c_y^{ref}(t)=\sum_{n=1}^{\infty}\frac{2AT_0^2\omega_n^2(1-\cos n\pi)}{n\pi(T_0^2\omega_n^2+n^2\pi^2)}\sin\left(\frac{n\pi}{T_0}t\right). \quad (13)$$

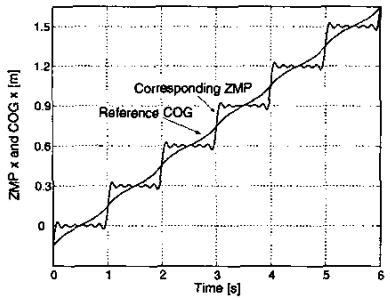

Fig. 4. Reference Trajectory of COG $c_x^{ref}(t)$ and Its Corresponding ZMP when $n = 12$

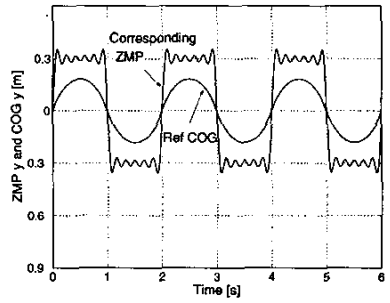

Fig. 5. Reference Trajectory of COG $c_y^{ref}(t)$ and Its Corresponding ZMP when $n = 12$

In fact, since these reference trajectories of equations (12) and (13) are composed of infinity series, we get the approximate solution with a positive constant n.

The resulting plots in Figures 4 and 5 show the effectiveness of the reference trajectory planning of COG by using approximate solution. In these figure, we used $\omega_n^2 = 10$ ($c_z = 0.9086[m]$ and $g = 9.806[m/s]$), $T_0 = 1[s]$, $A = 0.3[m]$, $B = 0.3[m]$ and $n = 12$. The corresponding ZMPs in figures represent the ZMPs generated by using approximate solution. In fact, we can express the difference between the reference ZMP in Figure 3 and the corresponding ZMP in Figures 4 and 5 as follows:

$$p_i^{ref} = c_i^{ref} - 1/\omega_n^2 \ddot{c}_i^{ref} + \delta, \tag{14}$$

where δ is the difference between the reference ZMP and corresponding ZMP. As n increases, the difference δ becomes smaller. Also, it is known that δ is the bounded value, $|\delta| < \beta$, for $i = x, y$, where β is a positive constant. The reference trajectories (12) and (13) of COG with a constant n will be used for the indirect ZMP controller in the following section.

IV. Indirect ZMP Control Law

Since a biped walking robot system is an electro-mechanical system including many electric motors, gears and link mechanisms, there exist many disturbances in executing the motions of the pre-generated reference trajectories of COG and ZMP for a real biped robot system. To

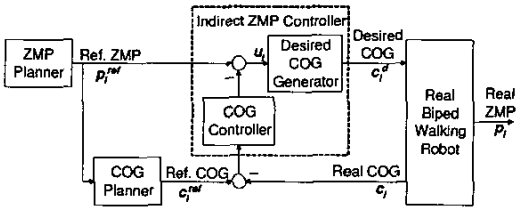

Fig. 6. Indirect ZMP Controller for a Biped Walking Robot

show the robustness of the controller against disturbances, we apply the following stability to a biped robot control system. The control system is said to be disturbance input-to-state stable (ISS) [13], if there exists a smooth positive definite radially unbounded function $V(\boldsymbol{x}, t)$, a class $\mathcal{K}_\infty$ function γ_1 and a class $\mathcal{K}$ function γ_2 such that the following dissipativity inequality is satisfied:

$$\dot{V} \leq -\gamma_1(|\boldsymbol{x}|) + \gamma_2(|\boldsymbol{d}|), \tag{15}$$

where $\dot{V}$ represents the total derivative for Lyapunov function, $\boldsymbol{x}$ state vector and $\boldsymbol{d}$ disturbance input vector.

In this section, we propose the indirect ZMP controller for biped robot systems as shown in Figure 6. In this figure, first, the ZMP Planer generates the reference trajectories (10) and (11). Second, the COG Planer generates the reference trajectories (12) and (13) with a suitable positive constant n. Third, we assume that the Desired COG Generator has the following form by using the state space equation (8):

$$\frac{d}{dt}\begin{bmatrix} c_i^d \\ \dot{c}_i^d \end{bmatrix} = \begin{bmatrix} 0 & 1 \\ \omega_n^2 & 0 \end{bmatrix}\begin{bmatrix} c_i^d \\ \dot{c}_i^d \end{bmatrix} + \begin{bmatrix} 0 \\ -\omega_n^2 \end{bmatrix} u_i, \tag{16}$$

where $\omega_n^2 = g/c_z^d$, c_i^d is the desired trajectory of COG and u_i is the ZMP control input, for $i = x, y$. Notice that this equation can also be expressed as $c_i^d - 1/\omega_n^2 \ddot{c}_i^d = u_i$. Fourth, the real biped walking robot has the following dynamics:

$$\begin{aligned} c_i &= c_i^d + \epsilon_i \\ p_i &= c_i - 1/\omega_n^2 \ddot{c}_i \quad \text{for} \quad i = x, y, \end{aligned} \tag{17}$$

where ϵ_i is the real control error, c_i and p_i are the real positions of COG and ZMP of the real biped robot, respectively. Note that the control error always exists in real robot systems and its magnitude depends on the performance of embedded local servos. In addition, we assume that the ZMP disturbance ($\eta \triangleq \epsilon_i - 1/\omega_n^2 \ddot{\epsilon}_i$) produced by the control error is bounded and its differentiation is also bounded, in other words, $|\eta| < a$ and $|\dot{\eta}| < b$ for positive constants a and b. The following theorem proves the stability of the indirect ZMP controller for a real biped walking robot.

Theorem 1: Let us define the ZMP and COG error for the real biped walking robot (17) as follows:

$$\begin{aligned} e_p &\triangleq p_i^{ref} - p_i \\ e_c &\triangleq c_i^{ref} - c_i. \end{aligned}$$

If the ZMP control input u_i in Figure 6 has the following form:

$$u_i = p_i^{ref} - \frac{1}{\omega_n^2}\left[2\zeta\gamma\dot{e}_c + (\gamma^2+\omega_n^2)e_c\right] \quad (18)$$

under the gain conditions:

$$\gamma > \frac{\omega_n}{\sqrt{(4-\alpha^2)\zeta^2-1}} \quad \text{and} \quad \frac{1}{\sqrt{4-\alpha^2}} < \zeta \leq 1, \quad (19)$$

for $0 < \alpha < \sqrt{3}$, then the indirect ZMP controller in Figure 6 gives the disturbance input$(\eta, \dot{\eta}, \delta)$-to-state$(e_p, e_c)$ stability (ISS) to a real biped walking robot.

Proof. First, we get the ZMP error dynamics from equations (14) and (17) as follows:

$$\ddot{e}_c = \omega_n^2(e_c - e_p + \delta). \quad (20)$$

Second, we obtain another ZMP error dynamics by using equations (16), (17) and (18) as follows:

$$e_p = 1/\omega_n^2\left(2\zeta\gamma\dot{e}_c + (\gamma^2+\omega_n^2)e_c\right) - \eta, \quad (21)$$

also, this equation can be rearranged for $\dot{e}_c$:

$$\dot{e}_c = 1/(2\zeta\gamma)\left(\omega_n^2 e_p - (\gamma^2+\omega_n^2)e_c + \omega_n^2\eta\right). \quad (22)$$

Third, by differentiating the equation (21) and by using equations (20) and (22), we get the following:

$$\begin{aligned}
\dot{e}_p &= 1/\omega_n^2\left(2\zeta\gamma\ddot{e}_c + (\gamma^2+\omega_n^2)\dot{e}_c\right) - \dot{\eta} \\
&= 2\zeta\gamma(e_c - e_p + \delta) \\
&\quad + \frac{\gamma^2+\omega_n^2}{2\zeta\gamma\omega_n^2}\left(\omega_n^2 e_p - (\gamma^2+\omega_n^2)e_c + \omega_n^2\eta\right) - \dot{\eta} \\
&= \left(2\zeta\gamma - \frac{(\gamma^2+\omega_n^2)^2}{2\zeta\gamma\omega_n^2}\right)e_c - \left(2\zeta\gamma - \frac{\gamma^2+\omega_n^2}{2\zeta\gamma}\right)e_p \\
&\quad + 2\zeta\gamma\delta + (\gamma^2+\omega_n^2)/(2\zeta\gamma)\eta - \dot{\eta} \\
&= \frac{(4\zeta^2\gamma^2\omega_n^2 - (\gamma^2+\omega_n^2)^2)}{2\zeta\gamma\omega_n^2}e_c \\
&\quad - \frac{(4\zeta^2\gamma^2 - (\gamma^2+\omega_n^2))}{2\zeta\gamma}e_p + d \qquad (23)
\end{aligned}$$

where $d \triangleq 2\zeta\gamma\delta + (\gamma^2+\omega_n^2)/(2\zeta\gamma)\eta - \dot{\eta}$. Fourth, let us consider the following Lyapunov function:

$$V(e_c, e_p) \triangleq (\zeta\gamma)e_c^2 + \frac{\zeta\gamma\omega_n^4}{(\gamma^2+\omega_n^2)^2 - 4\zeta^2\gamma^2\omega_n^2}e_p^2, \quad (24)$$

where $V(e_c, e_p)$ is the positive definite function for $0 < \zeta \leq 1$ except $e_c = 0$ and $e_p = 0$. Now, let us differentiate the above Lyapunov function

$$\begin{aligned}
\dot{V} &= 2(\zeta\gamma)e_c\dot{e}_c + \frac{2\zeta\gamma\omega_n^4}{(\gamma^2+\omega_n^2)^2 - 4\zeta^2\gamma^2\omega_n^2}e_p\dot{e}_p \\
&= \omega_n^2 e_c e_p - (\gamma^2+\omega_n^2)e_c^2 + \omega_n^2 e_c\eta \\
&\quad - \omega_n^2 e_p e_c - \frac{\omega_n^4[4\zeta^2\gamma^2 - (\gamma^2+\omega_n^2)]}{(\gamma^2+\omega_n^2)^2 - 4\zeta^2\gamma^2\omega_n^2}e_p^2 \\
&\quad + \frac{2\zeta\gamma\omega_n^4}{(\gamma^2+\omega_n^2)^2 - 4\zeta^2\gamma^2\omega_n^2}e_p d \\
&= -(\gamma^2+\omega_n^2)e_c^2 - \frac{\omega_n^4[4\zeta^2\gamma^2 - (\gamma^2+\omega_n^2)]}{(\gamma^2+\omega_n^2)^2 - 4\zeta^2\gamma^2\omega_n^2}e_p^2 \\
&\quad + \omega_n^2 e_c\eta + \frac{2\zeta\gamma\omega_n^4}{(\gamma^2+\omega_n^2)^2 - 4\zeta^2\gamma^2\omega_n^2}e_p d \\
&= -(\gamma^2+\omega_n^2)e_c^2 - \frac{\omega_n^4[4\zeta^2\gamma^2 - (\gamma^2+\omega_n^2)]}{(\gamma^2+\omega_n^2)^2 - 4\zeta^2\gamma^2\omega_n^2}e_p^2 \\
&\quad + \omega_n^2\left(e_c^2 - \left|e_c - \frac{1}{2}\eta\right|^2 + \frac{1}{4}\eta^2\right) \\
&\quad + \frac{\omega_n^4}{(\gamma^2+\omega_n^2)^2 - 4\zeta^2\gamma^2\omega_n^2} \times \\
&\quad \left(\alpha^2\zeta^2\gamma^2 e_p^2 - \left|\alpha\zeta\gamma e_p - \frac{1}{2\alpha}d\right|^2 + \frac{1}{4\alpha^2}d^2\right) \\
&= -\gamma^2 e_c^2 - \frac{\omega_n^4[(4-\alpha^2)\zeta^2\gamma^2 - (\gamma^2+\omega_n^2)]}{(\gamma^2+\omega_n^2)^2 - 4\zeta^2\gamma^2\omega_n^2}e_p^2 \\
&\quad - \omega_n^2\left|e_c - \frac{1}{2}\eta\right|^2 + \frac{\omega^2}{4}\eta^2 \\
&\quad - \frac{\omega_n^4}{(\gamma^2+\omega_n^2)^2 - 4\zeta^2\gamma^2\omega_n^2}\left|\alpha\zeta\gamma e_p - \frac{1}{2\alpha}d\right|^2 \\
&\quad + \frac{\omega_n^4}{4\alpha^2[(\gamma^2+\omega_n^2)^2 - 4\zeta^2\gamma^2\omega_n^2]}d^2
\end{aligned}$$

Since $d = 2\zeta\gamma\delta + (\gamma^2+\omega_n^2)/(2\zeta\gamma)\eta - \dot{\eta}$, if we apply the Schwartz inequality ($|a+b+c|^2 \leq 3|a|^2 + 3|b|^2 + 3|c|^2$) to d^2 term, then we get the following inequality:

$$\begin{aligned}
\dot{V} &\leq -\gamma^2 e_c^2 - \frac{\omega_n^4[(4-\alpha^2)\zeta^2\gamma^2 - (\gamma^2+\omega_n^2)]}{(\gamma^2+\omega_n^2)^2 - 4\zeta^2\gamma^2\omega_n^2}e_p^2 \\
&\quad + \frac{\omega^2}{4}\eta^2 + \frac{\omega_n^4}{4\alpha^2[(\gamma^2+\omega_n^2)^2 - 4\zeta^2\gamma^2\omega_n^2]}d^2 \\
&\leq -\gamma^2|e_c|^2 - \frac{\omega_n^4[(4-\alpha^2)\zeta^2\gamma^2 - (\gamma^2+\omega_n^2)]}{(\gamma^2+\omega_n^2)^2 - 4\zeta^2\gamma^2\omega_n^2}|e_p|^2 \\
&\quad + \left(\frac{\omega_n^2}{4} + \frac{3\omega_n^4(\gamma^2+\omega_n^2)^2}{16\alpha^2\zeta^2\gamma^2[(\gamma^2+\omega_n^2)^2 - 4\zeta^2\gamma^2\omega_n^2]}\right)|\eta|^2 \\
&\quad + \frac{12\omega_n^4\zeta^2\gamma^2}{4\alpha^2[(\gamma^2+\omega_n^2)^2 - 4\zeta^2\gamma^2\omega_n^2]}|\delta|^2 \\
&\quad + \frac{3\omega_n^4}{4\alpha^2[(\gamma^2+\omega_n^2)^2 - 4\zeta^2\gamma^2\omega_n^2]}|\dot{\eta}|^2, \qquad (25)
\end{aligned}$$

where $|e_p|^2$ term is negative definite under the given conditions (19). Therefore, since the inequality (25) follows the ISS property (15), we concludes that the indirect ZMP controller gives the disturbance input$(\eta, \dot{\eta}, \delta)$-to-state$(e_p, e_c)$ stability (ISS) to a real biped walking robot. □

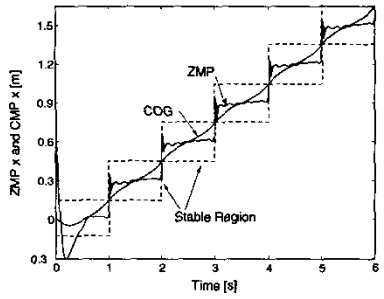

Fig. 7. Simulation Result : Real ZMP $p_x(t)$ and COG $c_x(t)$

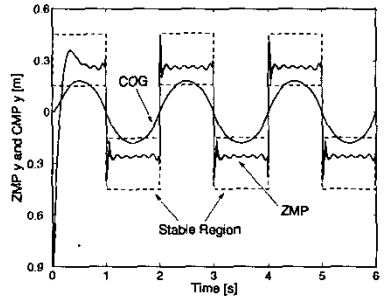

Fig. 8. Simulation Result : Real ZMP $p_y(t)$ and COG $c_y(t)$

Remark 1: In Figure 6, the COG Controller is a simple PD (Proportional-Derivative) controller as follows:

$$\frac{1}{\omega_n^2}\left[2\zeta\gamma\dot{e}_c + (\gamma^2+\omega_n^2)e_c\right].$$

In addition, since we get the COG error dynamics by using (20) and (21) as:

$$\ddot{e}_c + 2\zeta\gamma\dot{e}_c + \gamma^2 e_c = \omega_n^2(\delta - \eta),$$

we can prove the disturbance input(δ,η)-to-state$(e_c,\dot{e}_c)$ stability for a real biped walking robot.

In order to demonstrate the effectiveness of indirect ZMP controller proposed in this section, we simulated the controller using the reference trajectory of COG from Figures 4 and 5. If we set $\alpha = 1$ and $\zeta = 0.707$, the controller gain condition of (19) becomes

$$\gamma > \sqrt{20}.$$

With $\gamma = 10$, we get the resulting trajectories for ZMP and COG as shown in Figures 7 and 8. For large initial conditions ($p_x(0) = 0.9[m]$ and $p_y(0) = 0.9[m]$), these simulation results demonstrate the stability and robustness of the indirect ZMP controller while following the reference trajectories.

V. Concluding Remarks

In this paper, the reference COG trajectory planning method and the indirect ZMP control method were proposed for biped walking robots. The disturbance input-to-state stability (ISS) of the proposed indirect ZMP controller was proved to show the robustness against disturbances. Finally, we showed the effectiveness of the proposed indirect ZMP controller in simulations.

Acknowledgement

I would like to express the special thank to Dr. Doik Kim for his helpful discussion about dynamic simulation for humanoid robot.

References

[1] S. Kajita, F. Kanehiro, K. Kaneko, K. Fujiwara, K. Yokoi, and H. Hirukawa, "A realtime pattern generator for biped walking," *Proc. of IEEE Int. Conf. on Robotics and Automation*, pp. 31–37, 2002.

[2] A. Takanishi, H. Lim, M. Tsuda, and I. Kato, "Realization of dynamic biped walking stabilized by trunk motion on a sagittally uneven surface," *Proc. of IEEE/RSJ Int. Conf. on Intelligent Robots and Systems*, pp. 323–330, 1990.

[3] S. Kajita, F. Kanehiro, K. Kaneko, K. Fujiwara, K. Harada, K. Yokoi, and H. Hirukawa, "Biped walking pattern generation by using preview control of zero-moment point," *Proc. of IEEE Int. Conf. on Robotics and Automation*, pp. 1620–1626, 2003.

[4] T. Sugihara, Y. Nakamura, and H. Inoue, "Realtime humanoid motion generation through ZMP manipulation based on inverted pendulum control," *Proc. of IEEE Int. Conf. on Robotics and Automation*, pp. 1404–1409, 2002.

[5] J. H. Park, "Impedance control for biped robot locomotion," *IEEE Trans. on Robotics and Automation*, vol. 17, no. 6, pp. 870–882, Dec. 2001.

[6] J. H. Kim, S. W. Park, I. W. Park, and J. H. Oh, "Development of a humanoid biped walking robot platform KHR-1 - initial design and its performance evaluation," *Proc. 3rd IARP Int. Workshop on Humanoid and Human Friendly Robotics*, pp. 14–21, 2002.

[7] S. Kajita, T. Nagasaki, K. Yokoi, K. Kaneko, and K. Tanie, "Running pattern generation for a humanoid robot," *Proc. of IEEE Int. Conf. on Robotics and Automation*, pp. 2755–2761, 2002.

[8] T. Nagasaki, S. Kajita, K. Yokoi, K. Kaneko, and K. Tanie, "Running pattern generation and its evaluation using a realistic humanoid model," *Proc. of IEEE Int. Conf. on Robotics and Automation*, pp. 1336–1342, 2003.

[9] S. Kajita, F. Kanehiro, K. Kaneko, K. Fujiwara, K. Harada, K. Yokoi, and H. Hirukawa, "Resolved momentum control : Humanoid motion planning based on the linear and angular momentum," *Proc. of IEEE Int. Conf. on Robotics and Automation*, pp. 1644–1650, 2003.

[10] K. Harada, S. Kajita, K. Kaneko, and H. Hirukawa, "ZMP analysis for arm/leg coordination," *Proc. of IEEE Int. Conf. on Robotics and Automation*, pp. 75–81, 2003.

[11] E. R. Westervelt, J. W. Grizzle, and D. E. Koditschek, "Hybrid zero dynamics of planar biped walkers," *IEEE Trans. on Automatic Control*, vol. 48, no. 1, pp. 42–56, Jan. 2003.

[12] J. W. Grizzle, E. R. Westervelt, and C. Canudas de Wit, "Event-based PI control of a underactuated biped walker," *Proc., 42nd IEEE Conf. on Decision and Control*, pp. 3091–3096, 2003.

[13] Y. Choi and W. K. Chung, *PID Trajectory Tracking Control for Mechanical Systems*, vol. 298 of *Lecture Notes in Control and Information Sciences (LNCIS)*, Springer Publishing Co., 2004.